IOPscience iopscience.iop.org

Home Search Collections Journals About Contact us My IOPscience

Lattice dynamics of alpha -quartz. I. Experiment

This article has been downloaded from IOPscience. Please scroll down to see the full text article.

1993 J. Phys.: Condens. Matter 5 6149

(http://iopscience.iop.org/0953-8984/5/34/003)

View the table of contents for this issue, or go to the journal homepage for more

Download details:
IP Address: 171.66.16.159
The article was downloaded on 12/05/2010 at 14:21

Please note that terms and conditions apply.

J. Phys.: Condens. Matter 5 (1993) 6149–6154. Printed in the UK

Lattice dynamics of α-quartz: I. Experiment

D Strauch† and B Dorner‡

† Institut für Theoretische Physik, Universität, D-93053 Regensburg, Federal Republic of Germany

‡ Institut Laue-Langevin, F-38042 Grenoble Cedex, France

Received 22 April 1993, in final form 16 June 1993

Abstract. Using inelastic neutron scattering we have determined seven out of the nine dispersion branches of each of the Δ_1, Δ_2 and Δ_3 representations for wavevectors along the threefold screw axis as well as the 13 branches of the T_1 symmetry along the twofold axis. Strong dispersion occurs even in some of the highest-frequency branches.

1. Introduction

The bonding between silicon and oxygen is a subject of continuing interest, both from the experimental and theoretical points of view. On the one hand, SiO_2 exists in the glass state as well as in a variety of crystalline phases, and considerable effort is devoted to the study of these phases as well as their transitions [1, 2]. On the other hand, oxygen is the primary impurity in amorphous as well as crystalline silicon, and total-energy calculations [3–5] have shown that the Si–O–Si bonds of the oxygen impurities in silicon networks are very similar to the ones in crystalline and amorphous SiO_2. As the bonding is reflected in the vibrational spectra we undertook a detailed study of the lattice dynamics of α-quartz as a representative of an SiO_2 network.

Inelastic neutron scattering experiments have been carried out previously by Elcombe [6] in the Δ direction (Γ–A) and by Dorner and co-workers [7] in the T (Γ–K–M) and Σ (Γ–M) direction. The Brillouin zone of quartz with the standard notation of special points is shown in figure 1. These experiments had been restricted to frequencies below 8 THz. Joffrin and co-workers [8] have investigated the long-wavelength acoustic modes in the Γ–A direction, and Boysen and co-workers [9] have studied the soft modes at the M point. The dynamics near the α–β phase transition has been investigated by Bethke and co-workers [1]. We have extended the measurements in the Δ and T directions up to the highest frequencies. The experimental details will be given in section 2. Section 3 contains the results.

In the course of the present experiments it has turned out that the higher-frequency modes are rather poorly reproduced by previous model predictions [6, 10, 11]. A preliminary account of this work has been published elsewhere [12].

2. Experiment

The experiments have been performed on the instrument IN8 for frequencies up to 22 THz and on IN1 for frequencies between 7–40 THz. For the lower frequencies IN1 was used mainly when a large momentum transfer was required. Constant-Q scans have been recorded

0953-8984/93/346149+06$07.50 © 1993 IOP Publishing Ltd

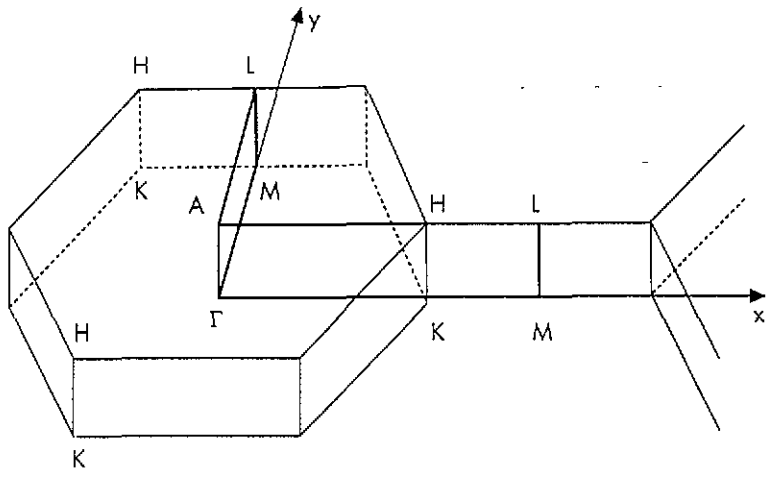

Figure 1. The upper half of the Brillouin zone of quartz with standard notation; after Barron and co-workers [10].

with the final momentum fixed at $k_f = 4.1\,\text{Å}^{-1}$ (IN8) and $k_f = 6.2\,\text{Å}^{-1}$ (IN1). Various collimations have been used in order to achieve a satisfactory resolution over the whole energy range. A graphite filter was mounted in front of the analyser of the instrument IN8 in order to reduce higher-order contamination.

The hydrothermally grown crystal of cylindrical shape (5 cm height, 4 cm diameter) was mounted in a Displex cryostat and kept at about 20 K. At this temperature the background (multiphonon) scattering was drastically reduced as compared to that at room temperature.

With three SiO_2 formula units in the primitive cell of quartz there are 27 phonon branches. Symmetry selection rules can be employed, and for momentum transfer in the Γ–A (z) direction the phonons of either one of the Δ_1, Δ_2 or Δ_3 representation (nine branches each) contribute to the cross section; similarly, for momentum transfer in the Γ–K (x) direction phonons of T_1 symmetry (13 branches) contribute to the cross section, while the 14 branches of T_2 symmetry are invisible.

The data have been analysed by a least-squares Gauss plus constant-background fit. The peak centre has been taken as the phonon frequency, and the peak width times height as the scattering intensity (up to a normalizing factor). The frequencies are given in tables 1–4.

Table 1. Δ_1 phonon frequencies (in THz) in α-quartz at 20 K for wavevectors $q = [0, 0, \xi]$ along the Γ–A direction ([0, 0, 0.5] is the zone boundary).

ξ	ν_1	ν_2	ν_3	ν_4	ν_5	ν_6	ν_7	ν_8	ν_9
0.0	—	6.53	10.44	12.36	14.09	15.80	—	32.48	36.70
0.1	—	6.56	9.94	12.10	13.99	16.40	—	32.39	—
0.2	2.10	6.64	9.21	12.50	14.00	16.77	—	32.46	—
0.3	2.91	6.40	8.52	12.66	13.92	16.96	—	32.45	36.76
0.4	3.31	—	8.09	12.75	13.87	17.21	—	32.48	36.59
0.5	3.77	—	8.12	12.80	13.93	17.57	—	32.48	36.41

In inelastic neutron scattering experiments only limited attention is often given to the Q-resolution of the instrument. The underlying idea is that the gradient of the dispersion surface as well as the accompanying structure factor change only little within the volume defined

Table 2. Δ_2 phonon frequencies (in THz) in α-quartz at 20 K for wavevectors $q = [0, 0, \xi]$ along the Γ–A direction.

ξ	ν_1	ν_2	ν_3	ν_4	ν_5	ν_6	ν_7	ν_8	ν_9
0.0	—	3.84	7.95	11.82	13.50	20.91	23.85	32.16	34.86
0.1	—	3.76	8.26	—	—	20.23	—	—	35.29
0.2	1.86	3.71	—	—	—	19.57	—	—	35.55
0.3	3.30	3.82	8.38	—	—	18.88	—	—	35.82
0.4	3.70	4.38	8.42	13.14	14.00	18.12	—	—	36.15
0.5	3.77	—	8.12	12.80	13.93	17.57	—	32.48	36.41

Table 3. Δ_3 phonon frequencies (in THz) in α-quartz at 20 K for wavevectors $q = [0, 0, \xi]$ along the Γ–A direction.

ξ	ν_1	ν_2	ν_3	ν_4	ν_5	ν_6	ν_7	ν_8	ν_9
0.0	—	3.84	7.95	11.82	13.50	20.91	23.85	32.16	34.86
0.1	0.81	4.05	7.80	11.58	13.55	21.86	—	—	34.57
0.2	1.25	4.32	—	11.58	13.24	22.28	—	—	34.22
0.3	1.47	4.69	6.80	11.62	12.87	23.19	23.67	—	34.07
0.4	1.53	5.13	6.40	11.89	12.57	23.15	23.54	—	33.92
0.5	1.90	5.15	6.07	12.31	12.60	23.45	—	—	33.94

Table 4. T_1 phonon frequencies (in THz) in α-quartz at 20 K for wavevectors $q = [\xi, 0, 0]$ along the Γ–K–M direction ([0.5, 0, 0] is the M-point).

ξ	ν_1	ν_2	ν_3	ν_4	ν_5	ν_6	ν_7	ν_8	ν_9	ν_{10}	ν_{11}	ν_{12}	ν_{13}
0.0	—	3.84	6.21	7.95	10.68	12.03	13.92	15.27	20.91	24.21	32.55	34.86	37.05
0.05	—	—	—	8.12	10.76	12.16	14.1	16.09	—	—	32.66	35.50	37.40
0.10	1.95	4.52	6.53	8.55	10.13	12.43	13.90	16.10	—	24.60	32.74	35.00	37.10
0.15	—	—	6.60	8.94	9.83	12.80	13.73	16.15	22.13	24.53	—	—	—
0.20	3.07	5.66	6.79	9.08	10.00	12.63	13.64	16.29	22.08	24.75	32.66	35.50	37.00
0.25	—	6.05	6.86	8.77	10.60	12.40	13.78	16.70	22.31	24.88	32.54	36.13	—
0.30	3.81	6.17	6.83	8.79	11.21	12.22	13.88	16.94	22.60	24.60	32.60	35.50	—
0.35	—	6.13	6.9	—	11.60	12.00	14.13	17.70	22.50	24.29	—	—	—
0.40	4.27	5.90	7.06	—	11.12	12.39	14.18	18.67	22.43	24.29	32.63	35.00	—
0.45	—	—	7.26	—	10.59	12.60	14.27	19.10	21.90	24.35	—	—	—
0.50	4.29	5.48	7.22	—	10.30	12.76	14.20	19.30	21.60	24.50	33.00	35.00	—

by the resolution ellipsoid. However, this assumption is only justified under the condition that the size of the ellipsoid is very small on the scale on which the eigenfrequencies and eigenvectors change appreciably. Typically, the latter scale is given by the size of the Brillouin zone. This condition was only poorly fulfilled in our measurements in particular on IN1, leading to a small Q-dependent shift in the measured frequencies. As this effect influences the errors of the absolute value of the measured frequencies we consider an accuracy of 0.2 THz appropriate for most of the data points, although relative errors of frequencies determined at neighbouring points in reciprocal space are smaller. We have used the calculated instrumental resolution to determine close-lying frequencies even if they are unresolved in the experimental spectra. We have not been able to determine all of the branches near 23 and 32 THz in the Δ direction for reasons of lack of sufficient scattering intensity. The missing branches have eigenvectors whose components are oriented predominantly perpendicular to the Δ direction. In the geometry Q parallel to the Δ direction, which provides the selection rules mentioned above, these branches show therefore

small intensities.

3. Results

The resulting dispersion curves are shown in figures 2 and 3, where the extended zone scheme is used for the phonons of Δ symmetry. The low-frequency portion is in close agreement with the room-temperature data of Elcombe [6] and Dorner and co-workers [7]. The frequencies at the Γ point are slightly different from the optical data [13–15].

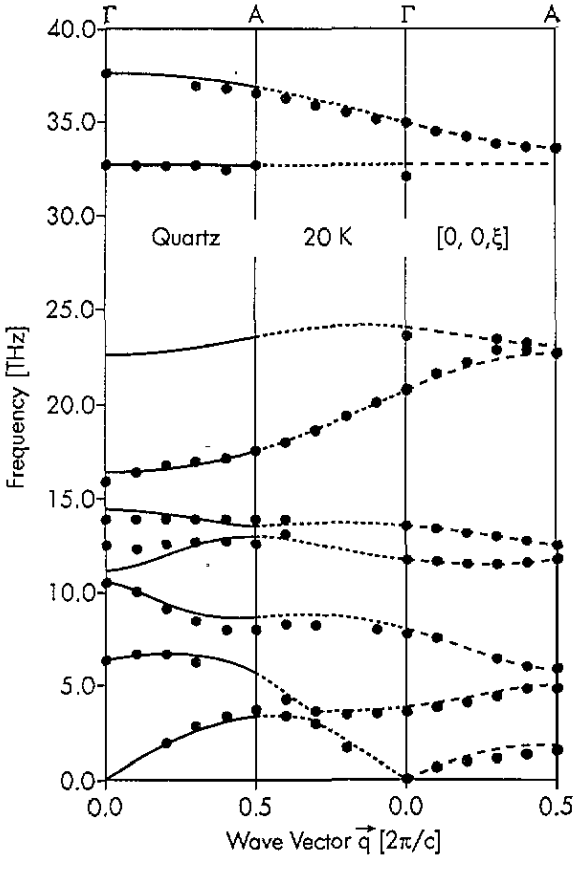

Figure 2. Dispersion curves of α-quartz at 20 K for the Γ–A direction. Symbols: experimental frequencies. Curves: theoretical results from shell model SM(4) (see the following paper). An extended-zone scheme is used to plot the dispersion curves for the three different irreducible representations separately.

Contrary to model predictions [6, 10, 11] some of the phonon dispersion curves in the high-frequency region exhibit a very strong dispersion. Likewise, model and experimental scattering intensities are at variance.

The scattering intensities indicate numerous areas in the energy–momentum space where there is an eigenvector exchange between different branches. Details will be discussed in the following paper [16], where the experimental dispersion curves will be analysed in terms of various models. As a result, quartz will turn out to be a strongly ionic crystal.

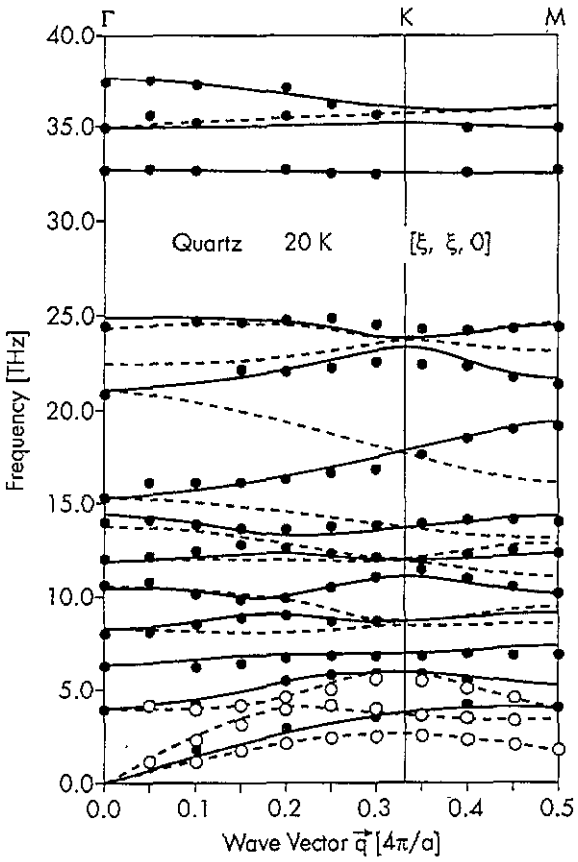

Figure 3. Dispersion curves of α-quartz at 20 K for the Γ–K–M direction. Symbols: experimental frequencies; closed circles, T_1 representation; open circles, T_2 representation (taken from Dorner and co-workers [7]). Curves: theoretical results from shell model SM(4) (see the following paper); —— T_1 representation; ····· T_2 representation.

Acknowledgments

We are grateful to H Schober for discussions.

References

[1] Bethke J, Dolino G, Eckold G, Berge B, Vallade M, Zeyen C M E, Hahn T, Arnold H and Moussa F 1987 *Europhys. Lett.* **3** 207
[2] Barrio R A, Galeener F L and Martinez E 1985 *Phys. Rev.* B **31** 7779
[3] Martinez E, Plans J and Yndurain F 1987 *Phys. Rev.* B **36** 8043
[4] Plans J, Diaz G, Martinez E and Yndurain F *Phys. Rev.* B **35** 788
[5] Ortega-Blake I, Tagüeña-Martinez J, Barrio R A, Martinez E and Yndurain F 1989 *Solid State Commun.* **71** 1107
[6] Elcombe M M 1967 *Proc. Phys. Soc.* **91** 947
[7] Dorner B, Grimm H and Rzany H 1980 *J. Phys. C: Solid State Phys.* **13** 6607
[8] Joffrin C, Dorner B and Joffrin J 1980 *J. Physique Lett.* **41** L-391
[9] Boysen H, Dorner B, Frey F and Grimm H 1980 *J. Phys. C: Solid State Phys.* **13** 6127

[10] Barron T H K, Huang C C and Pasternak A 1976 *J. Phys. C: Solid State Phys.* **9** 3925
[11] Striefler M E and Barsch G R 1975 *Phys. Rev.* B **12** 4553
[12] Dorner B, Strauch D, Schober H and Nützel K 1990 *Phonons 89* ed S Hunklinger, W Ludwing and G Weiss (Singapore: World Scientific) p 76
[13] Gervais F and Piriou B 1975 *Phys. Rev.* B **11** 3944
[14] Scott J F and Porto S P S 1967 *Phys. Rev.* **161** 903
[15] Fontanella J, Andeen C and Schuele D 1974 *J. Appl. Phys.* **45** 2852
[16] Schober H, Strauch D, Nützel K and Dorner B 1993 *J. Phys.: Condens. Matter* **5** 6155